

Method to Minimize Power Peaking in Refueling Schedule of Boiling Water Reactor

Hiroshi MOTODA and Osamu YOKOMIZO

*Atomic Energy Research Laboratory, Hitachi Ltd.**

Received May 12, 1976

Revised September 16, 1976

A method of optimizing fuel assembly allocation is proposed for a certain type of refueling schedule problem of Boiling Water Reactor (BWR) in which cycle length and number of fresh fuel assemblies to be loaded are predetermined.

The optimization is aimed at minimizing power peaking factor. The problem is decomposed into two subproblems: one to optimize the global region-wise shuffling scheme and the other to optimize assembly allocation. Linear programming is iteratively solved in the former subproblem such that the maximum excess reactivity is minimized and a direct search method is used in the latter subproblem.

The method is successfully applied to the 2nd and the 3rd cycle refueling schedule problems of a 460 MWe BWR. The optimized reloading patterns are compared with other non-optimal patterns which have much simpler or more symmetrical shuffling schemes. The optimization shows merit in reducing power peaking without sacrificing the cycle length.

KEYWORDS: *reactor fueling, power peaking, optimization, reactor cores, fuel, management, BWR type reactors, fuel assemblies, reactor operation*

I. INTRODUCTION

The primary objective of nuclear fuel management is to provide various principles required for the planning, scheduling, refueling, and safe and economical operations of nuclear power plants. In particular, the problem related to refueling schedule is referred to as in-core fuel management. This area has been studied by many investigators using various optimization techniques. The major researches are summarized in Refs. (1) and (2).

This paper discusses the problem of optimally allocating individual fuel assembly in a core. It is assumed that a long range optimization has been performed and the enrichment of reload fuels, number of assemblies to be loaded have been optimally determined elsewhere. These parameters can be determined without specifying the power distribution of each assembly. As is noted in Ref. (3), it is natural to separate the total in-core

fuel management problem into various sub-problems and to use objective functions, physical models of nuclear reactor and mathematical formulations which are appropriate to each sub-problem considering the phase at which it is located.

In this regard, the problem treated here fits one of the lowest levels, which is as important as the problems of higher levels because assembly by assembly location must have been specified before actual refueling takes place. Other main feature which supports the importance of this problem is that the main decision as to the number of assemblies to be loaded as well as the associated enrichment has generally been made long time before due to the required long lead time for fuel contracts and, therefore, the main interest left is to realize the power distribution as flat as possible under the

* *Ozenji, Tama-ku, Kawasaki.*

constraints of cycle length and other safety related problems.

II. OPTIMIZATION METHOD

1. Definition of Problem

The problem is to allocate the fuel assemblies in a core such that the radial power peaking is minimized under the following operational constraints:

- (1) The reactor has at least to assure a certain amount of cycle length.
- (2) The reactor has a certain stuck rod margin enough for reactor shutdown requirement at any burnup stage.
- (3) The reactor has to accept a certain amount of fresh reload fuel assemblies which have been purchased for the cycle, and their location in the core can be specified by utility's choice.
- (4) The reloading pattern must be realized within a certain amount of refueling steps.

The constraints (3) and (4) need explanation. General expression for the constraint (3) would be such that the amount of fresh reload assemblies must be less than or equal to a certain value. The first step of refueling schedule optimization is to determine this number, and here it is assumed that this number has been predetermined elsewhere to satisfy the inequality condition, as described in Chap. I. The problem treated in this paper is to use this as an equality constraint for the optimization of the lower level. It is understood that, in the constraint (4), the maximum allowable number of the refueling step should be determined by taking the balance of the two conflicting factors: the merits gained by the lower power peaking and the demerits caused by the lower capacity factor (increased down time). This relation is not clear at the moment, and the sensitivity analysis of this constraint is also one of the subjects.

Other constraints (ex. maximum burnup, maximum residence time *etc.*) which are listed in Ref. (1) are not repeated here.

2. Optimization Procedure

The optimization procedure is similar to that described in Ref. (1) in which the objective is to minimize the amount of fresh fuel to be loaded. It is basically divided into two sub-problems: one to optimize the global region-wise shuffling scheme and the other to optimize assembly allocation.

(1) Region-wise Shuffling

As in Ref. (1), fuel assemblies are leveled to include several assemblies of the same bundle type in each burnup level, and all the assemblies in the same level are assumed to have the same nuclear property. Fresh fuel assemblies are assigned to the first N_{type} levels (N_{type} : number of fuel bundle types).

The problem at this phase is to allocate these leveled assemblies to each region k in such a way that the global power peak is minimized. Let the number of assemblies of level l in region k be denoted as $x_{l,k}$, and the following linear programming (L.P.) formulation becomes possible. The meanings of the other variables are listed separately.

(a) Fresh fuel constraint

$$\sum_{k=1}^{N_{reg}} x_{l,k} = N_{amx_l}, \quad l=1, 2, \dots, N_{type} \quad (1)$$

$$N_{akmn_l,k} \leq x_{l,k} \leq N_{akmx_l,k}, \quad l=1, 2, \dots, N_{type} \\ k=1, 2, \dots, N_{reg} \quad (2)$$

(b) Continuity condition

$$\sum_{k=1}^{N_{reg}} x_{l,k} \leq N_{c_l}, \quad l=N_{type}+1, \dots, L \quad (3)$$

(c) Mass balance

$$\sum_{l=1}^L x_{l,k} = N_{asse_k}, \quad k=1, 2, \dots, N_{reg} \quad (4)$$

(d) Energy balance

$$\sum_{l=1}^L f_{l,k} x_{l,k} = N_{asse_k}, \quad k=1, 2, \dots, N_{reg} \quad (5)$$

(e) Reactivity balance

$$\sum_{l=1}^L k'_{\infty l,k} f_{l,k} x_{l,k} \geq N_{asse_k} k_{\infty k}^*, \quad k=1, 2, \dots, N_{reg} \quad (6)$$

(f) Performance index

$$J = \frac{\sum_{k=1}^{N_{reg}} P_k^{*A} \left(\sum_l k'_{\infty l,k} f_{l,k} x_{l,k} - N_{asse_k} k_{\infty k}^* \right)}{\sum_{k=1}^{N_{reg}} P_k^{*A}} \quad (7)$$

Equation (2) is to further specify the region-wise number of fresh fuel assemblies. If it is not desirable by some reason to place fresh reload fuel assemblies in some region k' , then $N_{akmn_{l,k}}$ and $N_{akmx_{l,k}}$ are set at zero for $k=k'$. Or, if the checker board loading is desired, then the $N_{akmn_{l,k}}$ and $N_{akmx_{l,k}}$ can be set at the corresponding number (ex. $1/4 \times$ number of assemblies in each region k). Of course this constraint can be excluded by setting $N_{akmn_{l,k}}=0$ and $N_{akmx_{l,k}}=\text{large number}$.

Contrary to the formulation in Ref. (1) (see Eq. (25) of Ref. (1)), the problem treated here requires inequality reactivity balance at EOC as shown in Eq. (6) to satisfy the constraint (1) because of the newly added constraint (3). The constraint (1) places a lower bound on the region-wise reactivity. The performance index of Eq. (7) stands for the excess reactivity and is related to Eq. (6). It is best to maximize the excess reactivity to automatically discharge the assemblies from the lowest k_{∞} . Furthermore, to maximize the excess reactivity gives the degree of freedom to further flatten the global power peak by modifying the target $k_{\infty,k}^*$ which appears on the right-hand side of reactivity balance equation (Eq. (6)).

Now, the problem can be stated as follows. First, estimate the EOC target power distribution by two-dimensional thermal hydraulic coupled calculation described in Ref. (3), and obtain P_k^* , $k_{\infty,k}^*$, U_k^* and F_k^* . Using these quantities, next estimate the EOC infinite multiplication factor $k_{\infty,l,k}^*$ and the assembly mismatch factor $f_{l,k}$ by the method similar to that described in Ref. (1). Since now the coefficients of L.P. have been obtained, solve the L.P. for $x_{l,k}$. Then, using the degree of freedom for fuel shuffling gained by the maximization of the excess reactivity, improve the EOC target distribution by iteratively re-distributing the region averaged exposure distribution. Physical insight indicates that the global power peaking can be further reduced by placing the more reactive fuel (*i.e.* fuel of higher importance) to the region near core periphery. This can be attained at the expense of the net reactivity. In other words, the region-wise shuffling

optimization here presented is to minimize the maximized excess reactivity. When the optimal target distribution has been found, the maximized excess reactivity is exactly zero in which case the resultant $x_{l,k}$'s satisfy the equality in Eq. (6) and J of Eq. (7) becomes zero. In this sense, Eq. (7) does not necessarily express the true net reactivity. The factor A used in Eq. (7) determines the degree of region-wise weighting P_k^{*A} and normally the value of A is chosen to be 2. Numerical experience, however, indicates the better performance of the solution for a negative value of A when the optimization procedure is terminated on the way.

The optimization of the EOC target distribution is based on the simple linear iterative search with one main and two sub-parameters included. Assuming the average exposure level of the central regions 1 (E_1) which is the first sub-parameter, criticality is attained by adjusting the average exposure level of the middle region $N_{regad}=[(N_{reg}+1)/2]$ for each value of the average exposure level of the outermost region $N_{reg}(E_{N_{reg}})$, which is a main parameter to be optimized. Average exposure levels of the other regions are obtained by smoothly interpolating the above three points by a distorted fourth order polynomial (Eq. (8)) which has the second sub-parameter φ to determine the degree of distortion.

$$\left. \begin{aligned} E_k &= (C_1 r_k^4 + C_2 r_k^2 + C_3)(1 + \varphi \sin y_k) \\ y_k &= C_4 \{r_k^2 - (C_5 + r_1)r_k + C_5 r_1\} \end{aligned} \right\} \quad (8)$$

The coefficients C_1 to C_5 are re-evaluated (see Appendix for the explicit expression of C_i) at each iteration of the criticality search. The requirement of the power flattening in the central region limits the range of the first sub-parameter E_1 . The second sub-parameter φ must be searched for parametrically.

For a reactor of N_{reg} regions, the degree of freedom of the target distribution ($E_1, E_2, \dots, E_{N_{reg}}$) is $N_{reg}-1$. To assume the shape of the target distribution to be of the modal expansion form shown in Eq. (8) limits the degree of freedom to three (one main parameter $E_{N_{reg}}$ and two sub-parameters E_1 and φ).

This makes the iterative procedure considerably simpler and the proper choice of these parameters covers wide range of target distributions. The criticality search is performed on the basis of the successive quadratic interpolation using the three latest pieces of data (*i.e.* the i -th guess $E_{N_{regad}}^i$ is determined by using $(E_{N_{regad}}^{i-1}, \lambda^{i-1})$, $(E_{N_{regad}}^{i-2}, \lambda^{i-2})$, $(E_{N_{regad}}^{i-3}, \lambda^{i-3})$ and λ_{target} (critical eigenvalue)).

The optimization procedure described here is shown in a simplified flow diagram of Fig. 1.

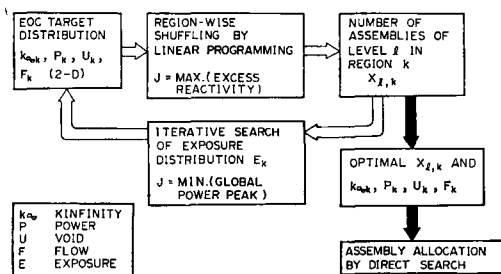


Fig. 1 Flow diagram of region-wise shuffling optimization

(2) Assembly Allocation

The direct search algorithm described Ref. (3) is used to optimize the assembly allocation using the optimal region-wise shuffling scheme as the constraint. Refueling steps are calculated to show in which order to discharge, shuffle, and load fresh fuel assemblies with minimum effort using the optimized allocation and the loading pattern of the previous cycle.

If the total amount of the refueling steps are larger than the limit, the steps are shortened in the following way. Assemblies are searched for in each of the refueling step chain: Discharge-Shuffle-Load and Store in the pool-Shuffle-Load. If there are more than two consecutive assemblies of the same type that have similar burnup at BOC (*i.e.* burnup difference ΔE_{stp}) in the chain, these shufflings are skipped from the first. The modification is repeated increasing the value of ΔE_{stp} until the constraint (4) is satisfied.

This relaxation makes the minimized power peak slightly larger.

The above functions have been added to the computer code OPREF.

III. RESULTS AND DISCUSSION

The refueling schedule of the 2nd and 3rd cycles of a commercial BWR of 460 MWe were generated placing the constraints on the location of the fresh reload fuel assemblies as well as on their total amounts. This seems to be the most probable situation encountered in actual practice.

1. Second Cycle Refueling Schedule

(1) Results

Fourteen assemblies (quarter core) were discharged from the largest burnup and the same amount of fresh reload Gd_2O_3 poisoned assemblies were loaded in a geometrical regular array (checker-board fashion). Proper shuffling of fuel assemblies is required because the locations of the assemblies to be discharged and to be loaded are different.

Figure 2 shows a simple out-in shuffling scheme. It is based on the shuffling of the assemblies which occupied the locations where the new fuel assemblies are to be loaded towards the core center region where the assemblies of the high burnup are to be discharged. This example was made by experience without much study (Case 2A). Figure 3 is the result obtained by OPREF⁽¹⁾ applied to the same problem (Case 2B₁), after implementing the functions described in Chap. II. It shows considerably complicated shuffling scheme compared with Case 2A. It seems difficult to make this complicated shuffling scheme by experience alone. Careful examination, however, reveals some rules out of the result. Many assemblies are moved outwards and those in the outer region are shuffled toward the core center. Figure 4 is the loading pattern which was generated by trial and error method after using this rule. The number of steps in one chain was limited to maximum three.

Table 1 summarizes the refueling characteristics of these three cases. Two cases are shown for the OPREF results. One is for the refueling step constraint of 80 (Case 2B₁) and the other for 100 (Case 2B₂).

(2) Discussion

Minimum number of refueling step requir-

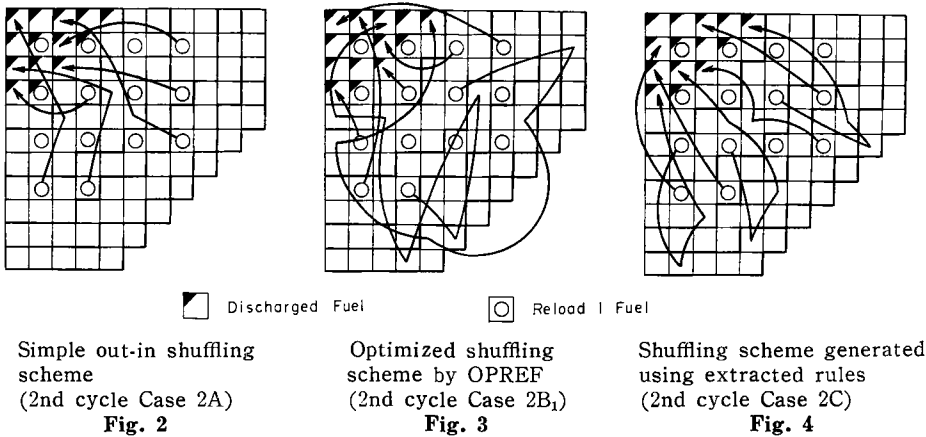


Table 1 Comparison of cycle length, power peak and refueling step for Case 2A, 2B and 2C

	Case 2A	Case 2B [†]		Case 2C
		B ₁	B ₂	
Cycle length (GWD/T)	5.01	5.26	5.28	5.12
Radial peak	1.36	1.35	1.34	1.37
Refueling step	46	80	100	54

[†] OPREF

ed is 39:14 for the discharge, 14 for the loading and 11 for the shuffling. Therefore, the step number of 46 of Case 2A is close to the minimum and there is little degree of freedom for the optimization by fuel shuffling.

Case 2B requires the lower limit of cycle length and the result depends on it. Here, the value of 5.3 GWD/T was chosen from the result of Case 2A. Case 2B₂ has the degree of freedom for shuffling which is 2.17 times as large as that of Case 2A and this could make the power peak reduced by 1.4%. The cycle length finally obtained was 5.28 GWD/T which is 0.4% smaller than the input value. This difference comes from the error of estimating $f_{l,k}$ and $k'_{\infty,k}$.

The optimization shows merit in reducing the power peak by 1.4% and increasing the cycle length by 5.4%. In Case 2B₁, where the refueling step constraint is reduced to 80, the power peak and the cycle length became worse by 0.9 and 0.4%, respectively than those of Case 2B₂. The reduction of the degree of freedom for shuffling necessitates

the increase of power peaking.

The dependence of the power peaking and the cycle length on the refueling step constraint is non-linear and shows reverse characteristics. Namely, the power peaking tends to saturate as the refueling step decreases, whereas the cycle length tends to saturate as it increases.

The shuffling scheme in Fig. 3 seems complicated at a glance. The principle lying behind is a balanced combination of the global k_{∞} distribution which makes the global power peak minimum and the local k_{∞} distribution which makes the assembly mismatching minimum. In Fig. 3, many assemblies are shuffled towards peripheral region and those in the peripheral region are shuffled inward.

Case 2C follows this rule with the maximum length of shuffling chain limited to three. The simplification resulted in the refueling steps of 54. The power peak became worse than that of Case 2A by 0.6%, the cycle length being longer by 2.2%. It is necessary to bring fuel assemblies of better nuclear property in the central core region to extend the cycle length. In Case 2C, this effect overwhelmed the effort of reducing the power peaking with the reduced refueling steps. A more complicated shuffling scheme is outside the scope of trial and error method. On the other hand, OPREF can automatically give the refueling schedule which is good enough in terms of power peaking and cycle length.

2. Third Cycle Refueling Schedule

(1) Results

Thirty three assemblies (quarter core) were discharged from the largest burnup, 14 assemblies discharged with lower burnup at EOC of the 1st cycle were reinserted and 19 fresh reload fuel assemblies were loaded. The fresh assemblies were arranged in a checker-board array.

Figure 5 is the reloading pattern which was generated by trial and error method (Case 3A). Emphasis was made on the geometrical symmetry of both fuel types and burnup to allocate assemblies in a scatter loading. In OPREF, the selection of the assemblies to be discharged and reinserted is obtained as the result of optimization. In general, the assemblies are discharged from the lowest k_{∞} and loaded from the largest k_{∞} . This concludes that the assemblies discharged at EOC of the 1st cycle should be all reinserted.

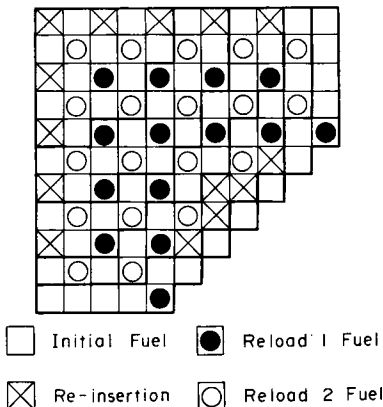


Fig. 5 Reloading pattern generated by trial and error method—Symmetry-oriented (3rd cycle Case 3A)

Figure 6 shows the convergence process of the region-wise shuffling optimization. The reactor core was divided into 5 regions and the exposure level of the outermost region 5 was varied as a main parameter. The two other sub-parameters were also investigated parametrically. The excess reactivity became nearly zero at the 5th iteration.

Figure 7 is the optimized reloading pattern obtained by the direct search using the converged region-wise shuffling scheme (Case

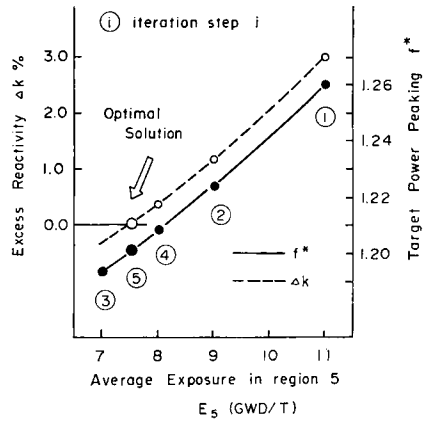


Fig. 6 Process of optimizing target distribution (3rd cycle Case 3B)

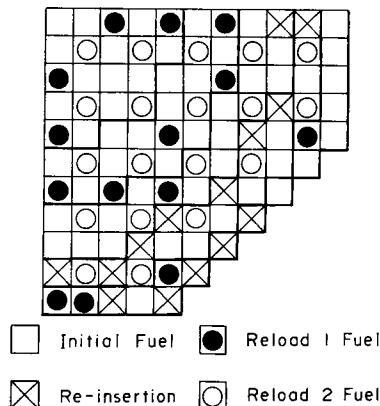


Fig. 7 Reloading pattern optimized by OPREF (3rd cycle Case 3B)

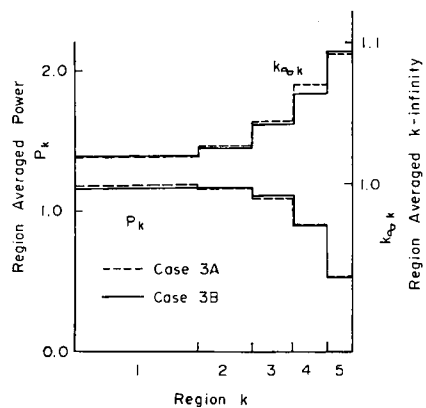


Fig. 8 Comparison of region averaged power and infinite multiplication factor for Cases 3A and 3B

3B). No constraint was imposed on the amount of refueling steps.

Figure 8 compares the region averaged power and infinite multiplication factor distributions of Case 3A and 3B. **Figure 9** shows the assembly power distributions in the second array from the core center line for both cases. Similar figures can be drawn in the other sections of the core.

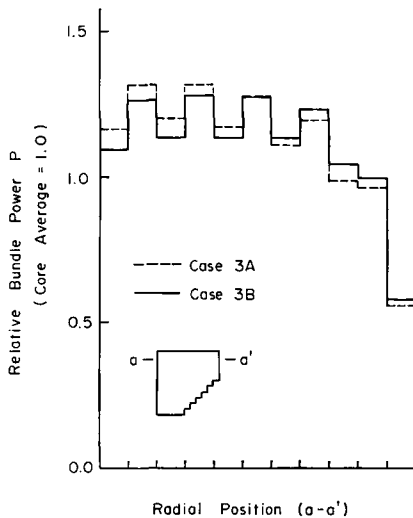


Fig. 9 Comparison of bundle power for Cases 3A and 3B

Table 2 summarizes the refueling characteristics of these two cases. The results of both two- and three-dimensional simulations are given.

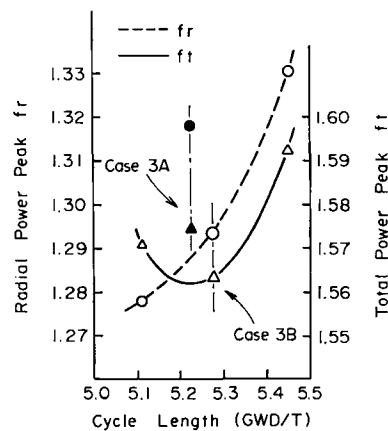
Table 2 Comparison of cycle length, power peak, MCHFR, stuck rod margin and refueling step for Cases 3A and 3B

	Case 3A		Case 3B	
	2-D	3-D	2-D†	3-D
Cycle length (GWD/T)	5.18	5.23	5.27	5.28
Radial peak (location)	1.33 (4, 8)	1.32 (4, 8)	1.31 (2, 6)	1.29 (2, 6)
Total peak (location)	1.57 (4, 8, 4)	1.57 (4, 8, 3)	1.54 (2, 6, 4)	1.56 (4, 6, 3)
MCHFR (location)	3.46 (4, 8, 9)	3.36 (2, 10, 10)	3.55 (2, 6, 9)	3.51 (2, 6, 9)
Stuck rod margin (%Δk)	1.7	1.6	1.3	1.3
Refueling step	116	116	134	134

† OPREF

Figure 10 shows the total power peaking and the radial power peaking of the opti-

mized refueling schedules by OPREF with the cycle length varied as a parameter. This results were obtained by three-dimensional simulation. In Fig. 10, the solid marks ● and ▲ indicate the results of Case 3A for reference.



The solid marks ● and ▲ indicate the results, f_r and f_t , of Case 3A for reference.

Fig. 10 Relation between power peak and cycle length

(2) Discussion

Fairly intricate shuffling scheme is required for the 3rd cycle because there exists the notable spread in the burnup distribution of the assemblies to be used. The minimum number of refueling steps is 80:33 for the discharge, 14 for the reinsection, 19 for the loading and 14 for the shuffling. The refueling steps of Case 3A is 116, the difference of which from the minimum required number is 5 times as large as that of Case 2A. The assemblies are beautifully arranged.

The input specified cycle length of Case 3B was also set at 5.3 GWD/T. It is seen that the power peaking of the target power distribution is reduced from 1.26 of the initial value to 1.20 of the optimized value. Naturally no feasible solution exists in the L.P. calculation at the 3rd iteration. It can be said that the optimization process has been completely converged because the maximized excess reactivity became nearly zero.

In the final result of Case 3B shown in Fig. 7, it is the fresh reload fuel assemblies (Reload 2 Fuel in the figure) alone that were

intentionally loaded in a checker-board array. However, almost all of the assemblies newly loaded at the 2nd cycle (Reload 1 Fuel) and those reinserted at this cycle (Re-Insertion) are placed in a geometrically symmetrical positions except those in the outermost two layers. The checker-board loading of the fresh fuel assemblies which occupy about $\frac{1}{5}$ of the core necessitates the symmetry of other assemblies in order to reduce the in-region assembly mismatching although the region averaged k_{∞} distribution at BOC is not uniform for both Case 3A and 3B as is easily estimated by the EOC k_{∞} distributions shown in Fig. 8. This does not apply for those in the outermost two layers.

The region-wise shuffling scheme has been determined in relation to the target k_{∞} distribution and thus, the region-wise loading fraction of the assemblies with similar exposure levels is not uniform throughout the core. If the locations of the fresh fuel assemblies had not been specified, the optimized solution may not have been symmetrical as was experienced in Ref.(3) and the power peaking could have been made smaller.

By comparing the results of Case 3A and 3B, it is noted that the radial power peaking f_r of Case 3B is 2.3% smaller, the total power peaking f_t 0.6% smaller and the cycle length 0.96% larger than the corresponding values of Case 3A. The reduction of the radial power peaking is worth noting and the optimization shows merit.

However, there is not much reduction in the total power peaking. This is solely because OPREF is based on two-dimensional calculation and cannot correctly evaluate the three-dimensional power peaking.

In Case 3A, the assembly of the maximum power is responsible for the largest power peak. This is not true for Case 3B. This means that the reduction of the radial power peaking is not necessarily equivalent to the reduction of the total power peaking in some cases. This is the drawback of two-dimensional analysis, which is clearly shown in Fig. 10. Whereas the radial power peaking f_r monotonically increases as the cycle length increases, the total power peaking f_t has a

minimum. At present only one standard axial power distribution is used to evaluate total power peak as well as to calculate the axial void and infinite multiplication factor distributions. This problem may be eliminated by introducing several standard axial power distributions (ex. fuel type-wise and burnup level-wise). However, further study is necessary to evaluate the effectiveness quantitatively.

The effect of power flattening of global power distribution is seen well in Figs. 8 and 9. Although considerable effort is made to reduce the power mismatching in Case 3A also, the slight difference of k_{∞} in the outer regions ($k=3, 4, 5$) causes the difference of the power level of the central flattened region. This, combined with the optimization by the direct search, reduces the assembly power as is shown in Fig. 9.

The shut-down margin of Case 3B is 19% smaller. The reactivity limit imposed on this constraint was $1\% \Delta k/k$ and the result is well under this limit. It could be possible to further strengthen this constraint because the location of the peak power assembly is not directly related to the control rod of maximum reactivity worth at cold shutdown. The refueling steps increased by 16% (18 steps). This may be considered acceptable since it only adds about half a day to the refueling operation.

In summary, the optimized pattern generated by OPREF has better performance characteristics than those obtained by trial and error method. It has dispensed with time consuming manual search. It is, however, felt desirable to include various empirical rules to make the result more acceptable for actual practice. It is noted that the result of OPREF can be used as the initial starting pattern for the more detailed analysis.

IV. CONCLUSIONS

A method of minimizing the power peaking is proposed for the refueling studies of BWR, in which the cycle length and the batch size of the newly loaded fresh assem-

blies are assumed to have been specified. This method has been applied to generate the 2nd and the 3rd cycle refueling schedule problems of a commercial BWR of 460 MWe.

- (1) It is possible by the method developed here to generate a refueling schedule which is advantageous over those obtained by carefully examined trial and error method in terms of power peaking and cycle length with other constraints keeping under the limits.
- (2) If the fresh fuel assemblies which occupy at least $\frac{1}{5}$ of the core are to be loaded in a checker-board array, the remaining assemblies are also to be arranged in a geometrically symmetrical locations in order to reduce the power peaking.
- (3) The reduction of the radial power peaking does not necessarily guarantee the reduction of the total power peaking in three-dimensional geometry. The solution to this problem has not yet been found.
- (4) Continuous effort is still required to improve the optimization functions and to make the result more practical by including the various know how which has so far been developed mostly on the basis of sound engineering judgement.

[NOMENCLATURE]

N_{type}	Number of fuel bundle types
N_{reg}	Number of regions
N_{c_l}	Number of assemblies in levelized burnup level l
L	Number of burnup levels
N_{amx_l}	Number of fresh fuel assemblies of type l
$N_{\text{akmn}_l, k}$	Minimum number of fresh fuel assemblies of type l to be loaded in region k
$N_{\text{akmx}_l, k}$	Maximum number of fresh fuel assemblies of type l to be loaded in region k
N_{asse_k}	Number of assemblies in region k
$f_{l, k}$	Estimated power mismatch factor of assemblies of level l in region k
$k'_{\text{ool}, k}$	Estimated EOC infinite multiplication factor of assemblies of level l in region k

$k'_{\infty, k}$	EOC target infinite multiplication factor in region k
P_k^*	EOC target power in region k
U_k^*	EOC target void in region k
F_k^*	EOC target flow in region k
A	Weighting constant
r_k	Normalized radius of region k (Distance from core center to middle of region k)
C_i	Fitting coefficients
φ	Distortion factor

ACKNOWLEDGMENTS

The authors wish to express their thanks to Drs. K. Taniguchi, S. Yamada and S. Kobayashi of Atomic Energy Research Laboratory, Hitachi Ltd., for their encouragement and support throughout this study. Acknowledgment is also due to Dr. H. Hiranuma of Hitachi Works, Hitachi Ltd., for his critical review of the manuscript.

—REFERENCES—

- (1) MOTODA, H., *et al.*: Optimization of refueling schedule for light water reactors, *Nucl. Technol.*, **25**, 477 (1975).
- (2) MINGLE, J.O.: In-core fuel management via perturbation theory, *ibid.*, **27**, 248 (1975).
- (3) MOTODA, H., YOKOMIZO, O.: Optimization of fuel assembly allocation for boiling water reactors, *J. Nucl. Sci. Technol.*, **13**[5], 230 (1976).

[APPENDIX]

The coefficients C_1 to C_5 used in Eq. (8) are given below.

$$C_1 = \frac{f-g}{r_1^2 - r_3^2}$$

$$C_2 = f - C_1(r_1^2 + r_3^2)$$

$$C_3 = E_1 - C_1 r_1 - C_2 r_1^2$$

$$C_4 = \frac{\pi}{(r_2 - r_1)(r_2 - C_5)}$$

$$C_5 = \frac{r_3^2 - r_1 r_3 - 2r_2^2 + 2r_2^2}{r_3 + r_1 - 2r_2}$$

where

$$f = \frac{E_1 - E_2}{r_1^2 - r_3^2}, \quad g = \frac{E_2 - E_3}{r_2^2 - r_3^2}$$

$$E_2 = E_{N_{\text{regad}}}, \quad E_3 = E_{N_{\text{reg}}}$$

$$r_2 = r_{N_{\text{regad}}}, \quad r_3 = r_{N_{\text{reg}}}$$

$$N_{\text{regad}} = [(N_{\text{reg}} + 1)/2]$$

$$r_k = \sqrt{\left(\sum_{k'=1}^k N_{\text{asse}_{k'}} - 0.5 N_{\text{asse}_k} \right) / \sum_{k'=1}^{N_{\text{reg}}} N_{\text{asse}_{k'}}}$$